Book Chapter

Optical and Morphological Properties of ZnO and TiO_2 Derived Nanostructures Synthesized via a Microwave-Assisted Hydrothermal Method

Nosipho Moloto[1], Siyasanga Mpelane[2], Lucky M Sikhwivhilu[3]* and Suprakas Sinha Ray[4,5]

[1]Molecular Sciences Institute, School of Chemistry, University of the Witwatersrand, Republic of South Africa
[2]Department of Chemistry, University of Johannesburg, South Africa
[3]DSI/Mintek Nanotechnology Innovation Centre, Advanced Materials Division, South Africa
[4]DSI/CSIR Nanotechnology Innovation Centre, National Centre for Nano-Structured Materials, Council for Scientific and Industrial Research, Republic of South Africa
[5]Department of Chemical Technology, University of Johannesburg, South Africa

***Corresponding Author:** Lucky M Sikhwivhilu, DSI/Mintek Nanotechnology Innovation Centre, Advanced Materials Division, Mintek, Private Bag X3015, Randburg, Johannesburg, 2125, South Africa

Published **September 24, 2020**

This Book Chapter is a republication of an article published by Lucky M Sikhwivhilu, et al. at International Journal of Photoenergy in February 2012. (Nosipho Moloto, Siyasanga Mpelane, Lucky M Sikhwivhilu, Suprakas Sinha Ray. Optical and Morphological Properties of ZnO- and TiO_2-Derived Nanostructures Synthesized via a Microwave-Assisted Hydrothermal Method. International Journal of Photoenergy. Volume 2012, Article ID 189069, 6 pages. doi:10.1155/2012/189069)

How to cite this book chapter: Nosipho Moloto, Siyasanga Mpelane, Lucky M Sikhwivhilu, Suprakas Sinha Ray. Optical and Morphological Properties of ZnO- and TiO_2-Derived Nanostructures Synthesized via a Microwave-Assisted Hydrothermal Method. In: Fan Xiao, editor. Advances in Energy Research: 2nd Edition. Hyderabad, India: Vide Leaf. 2020.

Acknowledgements: The authors would like to thank the Department of Science and Innovation (SA) and Mintek (Council for Mineral Technology - SA) for financial support.

Abstract

A microwave-assisted hydrothermal method was used to synthesize ZnO and TiO_2 nanostructures. The experimental results show that the method resulted in crystalline monodispersed ZnO nanorods that have pointed tips with hexagonal crystal phase. TiO_2 nanotubes were also formed with minimum bundles. The mechanism for the formation of the tubes was validated by HRTEM results. The optical properties of both ZnO and TiO_2 nanostructures showed characteristics of strong quantum confinement regime. The photoluminescence spectrum of TiO_2 nanotubes shows good improvement from previously reported data.

Keywords

ZnO, TiO_2, Microwave, Hydrothermal, Nanorods, Nanotubes, Quantum Confinement

Introduction

The fabrication of size and shape controlled nanoparticles and their assembly into materials still poses a challenge in the area of nanosciences. It is well recognized that the shape of the nanoparticles plays a crucial role in determining their resultant properties [1-5]. One of the difficulties associated with the synthesis of anisotropic nanoparticles is the control of growth through variation of the reaction parameters [6-10]. Factors such as concentration, temperature, pH, capping agent as well as the reaction time are critical parameters that influence the size and the morphology of the nanoparticles. Apart from these factors, altering a synthetic strategy can also introduce surprising results. Herein we report on the syntheses of ZnO and TiO_2 nanoparticles using a microwave assisted method. Their optical and morphological properties are also investigated.

ZnO has attracted much attention because of its outstanding physical properties. It is an II-VI semiconductor that has a direct wide band-gap of 3.37 eV and a large excitonic binding energy (60 meV). Because of these properties ZnO has found use in various technological applications including transparent conducting electrodes for solar cells, photocatalysis, surface acoustic devices, UV lasers and as chemical and biological sensors [11-15]. Various methods such as the sol-gel method, hydrothermal process, chemical vapour deposition and the single-source precursor method have been employed to synthesize different ZnO nanostructures [16-19]. Though similar to ZnO, TiO_2 has been found to be particularly very effective in photocalysis and has been employed in this capacity as an active layer in photovoltaics as well as an electrode in photoelectrolysis cells where it has been known to enhance the efficiency of electrolytic splitting of water into hydrogen and oxygen [20]. TiO_2 is a semiconductor with a structurally dependent band-gap (anatase - 3.20 eV and rutile – 3.03 eV) [21]. TiO_2 has been prepared via several techniques such as the sol-gel, hydrothermal process, and pulse laser deposition [22-24].

Although the sol-gel method is widely accepted for the preparation of both ZnO and TiO_2 nanostructures, the

calcinations process is essential and can cause further particle growth, induce phase transformation and result in lower specific surface area. The method also results in the incorporation of impurities and poor crystallinity [25]. In this context, the use of the microwave assisted method is expected to be an alternative to the sol-gel technique. The most notable effect of microwave irradiation is the heating effect. In microwave heating, unlike in conventional heating, heat is generated within the material itself instead of heat supplied from external sources. As a result of this internal and volumetric heating, thermal gradients and flow of heat during microwave processing are quite different from those observed in conventional heating. This heating mechanism also results in the reduction of the reaction time. The optical and morphological properties of ZnO and TiO_2 synthesized using the microwave-assisted method are hereby reported.

Experimental

Reagents

Titania (TiO_2, P25 Degussa), zinc oxide, potassium hydroxide, hydrogen peroxide and methanol were all purchased from Merck, South Africa. The potassium hydroxide (KOH) and hydrogen peroxide (H_2O_2) were diluted accordingly to obtain the desired concentration.

Synthesis of ZnO Derived Nanostructures

About 0.045 mol of ZnO powder was added to 20 ml of 30 % hydrogen peroxide. The solution was then placed in Teflon container and heated in a microwave oven with a maximum power of 1200 W, at a pressure of 30 bars for 15 min. The resultant particles were then washed several times with deionised water and dried in a conventional oven at 100 $^{\circ}$C for 5 h.

Synthesis of the TiO_2 Derived Nanostructures

In a typical synthesis, 22g of TiO_2 powder was added to a 200 ml of 18 M potassium hydroxide. The solution was then placed in Teflon container and heated in a microwave oven with a maximum power of 1200 W, at a pressure of 22 bars for 15 min.

The resultant particles were then washed several times with deionised water until the conductivity of the solution was below 100 µS/cm and finally dried in a conventional oven at 100 °C for 5 h.

Structural Characterization

X-ray diffraction: XRD patterns on powdered samples were measured on a Phillips X'Pert materials research diffractometer using secondary graphite monochromated Cu Kα radiation (λ = 1.54060 Å) at 40 kV/50 mA. Measurements were taken using a glancing angle of incidence detector at an angle of 2°, for 2θ values over 10° – 80° in steps of 0.05° with a scan speed of 0.01° $2\theta.s^{-1}$.

Electron microscopy: The samples were characterized using field emission scanning electron microscopy (FE-SEM)(Leo, Zeiss), operated at 3-10 kV electron potential difference and equipped with a semiconductor detector that allows for detection of energy dispersive X-rays (EDX). The samples were prepared by placing a thin layer of powder on a carbon tape. The high resolution transmission electron microscopy (HRTEM) was carried out on a Joel JEM-2100 microscopy with a LAB6 filament. The measurements were carried out at 200 kV with a beam spot size of 20 - 200 nm in TEM mode. The samples were prepared by placing a drop of particles suspended in methanol on a holey carbon coated copper grid.

Optical Characterization

Absorption spectroscopy: A Perkin Elmer Lambda 75S UV-VIS-NIR Spectrophotometer with double grating and double monochromator for high absorbance measurements was used to carry out the optical measurements. The powders were suspended in methanol and placed in quartz cuvettes (1 cm, path length). The band-edges of the samples were determined from absorption spectrum by extrapolation.

Emission spectroscopy: A Perkin Elmer LS55 with a xenon lamp (150 W) and a 152 P photo multiplier tube as a detector

was used to measure the photoluminescence of the particles. The samples were suspended in methanol and placed in quartz cuvettes (1-cm path length) for spectral analysis.

Results and Discussions

Morphological Properties

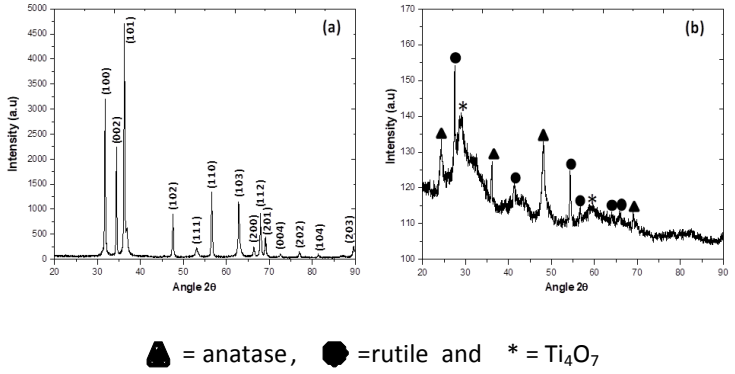

Figure 1: X-ray diffractograms of (a) ZnO and (b) TiO_2.

The XRD patterns of the as-synthesized ZnO and TiO_2 are shown in Figure 1(a) and (b) respectively. The diffraction peaks in Figure 1(a) could be indexed to a hexagonal phase ZnO (JCPDS 36-1451). The slight broadening of the peaks is ascribed to size effect. The diffraction pattern of titania depicted in Figure 1 (b), revealed the presence of both rutile (JCPDS 88-1175) and anatase (JCPDS 84-1286) phase. Two broad peaks belonging to neither rutile nor anatase were also detected. These peaks could be indexed to a titanate structure, Ti_4O_7. The titanate structures containing potassium ions, $KTiO_2(OH)$, have been previously observed and this was attributed to the intercalation of potassium ions into TiO_2 framework [26]. In the current study the use of microwave resulted in the formation of a titanate structure (Ti_4O_7) without potassium ions. This clearly shows that the intercalation of potassium ions is dependent on the time and method of processing. The crystallinity of the TiO_2 sample is slightly poorer when compared to that of ZnO and this is probably due to the difference in particle size and shape.

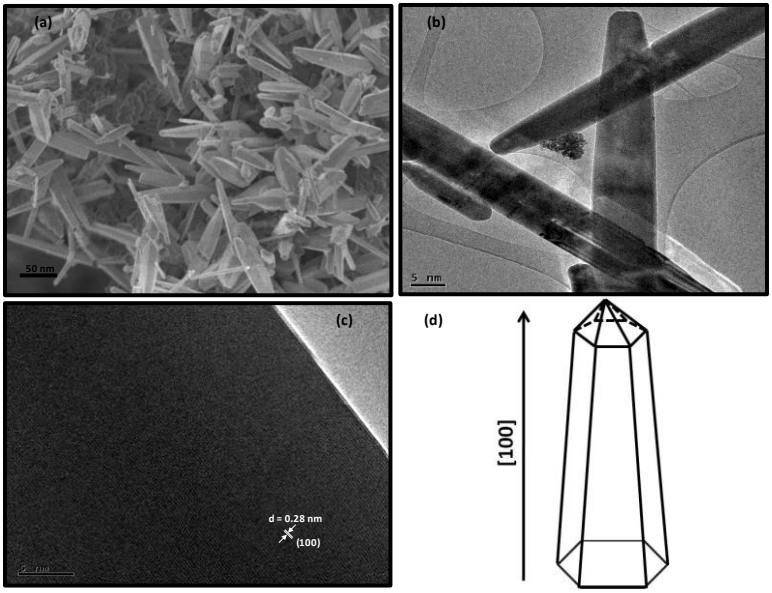

Figure 2: (a) SEM, (b) TEM, (c) HRTEM micrographs of ZnO and (d) sketch illustrating the shape of ZnO.

The morphologies of ZnO and TiO_2 nanostructures are depicted in Figure 2 and Figure 3 respectively. The SEM micrograph in Figure 2(a) shows rod-like nanostructures with pointed tips. The TEM image in Figure 2(b) confirms the morphology as that of pointed-tip rods. The particles have a very high aspect ratio. The averaged particle size was found to be 36 nm. The HRTEM depicted in Figure 2(c) shows a crystalline particle indicated by the presence of the lattice fringes with the lattice spacing (d = 0.28 nm) that could be indexed to a (100) crystal plane of hexagonal ZnO. This is in agreement with the observed crystal phase in Figure 1(a). The sketch in Figure 2(d) shows the perceived geometry of the particle with the rod growth occurring along the (100) plane as corroborated by the HRTEM.

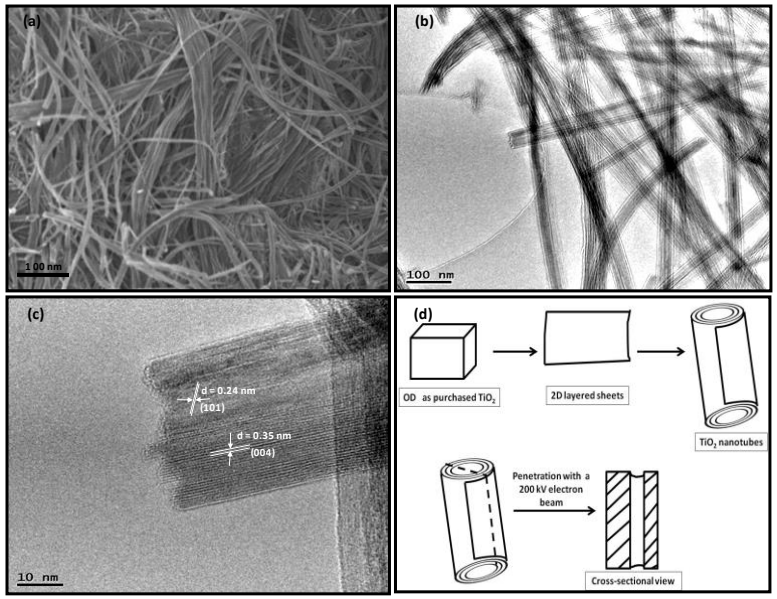

Figure 3: (a) SEM, (b) TEM, (c) HRTEM micrographs of TiO_2 and (d) formation mechanism of TiO_2 nanotubes.

The SEM image of TiO_2 in Figure 3(a) shows entangled nanotubular structures. The TEM confirms the morphology to be tubular rather than wires. The tubes show narrow size distribution with the diameters being approximately 25 nm. The HRTEM shown in Figure 3(c) shows a single tube with crystal fringes indexed to the anatase phase. The sizes of the walls of the tube appear to be asymmetrical. This is to be expected as various authors have suggested that the formation of the tubes as a mere rolling up of the TiO_2 sheets (Fig, 3(d)) [26,27]. This growth mechanism is clearly supported and confirmed in this case by the HRTEM image in Figure 3(c).

Optical Properties

Zinc oxide is a direct band gap semiconductor with bulk band gap energy of 3.37 eV (368 nm). The optical properties are shown in Figure 4(a). The band-edge is a function of the composition, size, and shape of the nanonocrystal. The absorption spectrum has a band-edge at 350 nm. The band –edge

is blue-shifted from bulk band-edge of 368 nm. This is indicative of quantum confinement of the exciton within the ZnO nanocrystal and this is characteristic of nanoparticles. Another impressive feature of semiconductor nanoparticles is their ability to emit light. Upon excitation with wavelength shorter or equivalent to the absorption onset, an electron is promoted from the valence band to the conduction band and upon relaxation a phonon of light is emitted. The emission spectrum of ZnO is depicted in Figure 4(a) shows a relatively narrow Gaussian distributed curve signifying a monodispersed particles population. The wavelength at maximum emission (420 nm) is red-shifted from the first absorption peak by a stoke shift of approximately 80 nm. The sharpness and the intensity of the peak suggest that the particles are very stable and have very few surface traps. The Stoke shift for the ZnO is particularly large. Stokes shift is well known both in the molecular spectroscopy and in the spectroscopy of the nanoparticles. It is known that this kind of shift (so-called Frank-Condon shift) is due to vibrational relaxation of the excited nanoparticles to the ground state [28].

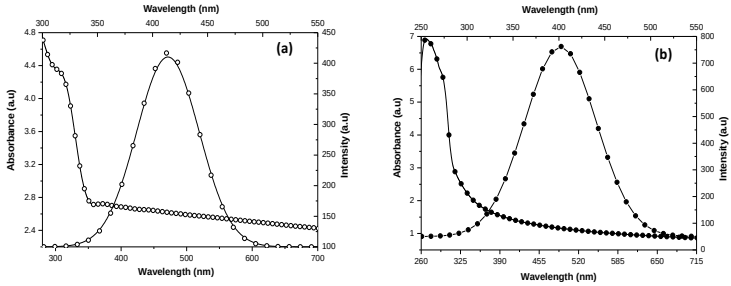

Figure 4: Absorption and emission spectra of (a) ZnO and (b) TiO_2.

The absorption spectrum of TiO_2 nanotubes in Figure 4(b) shows an absorption band-edge at 371 nm. This peak is blue-shifted from the bulk band-edge of 388 nm. Similarly to ZnO, this suggests strong quantum confinement of the excitons. The photoluminescence spectrum of TiO_2 usually shows poor characteristics probably because the hydrothermal and sol-gel methods usually used to synthesize the nanostructures do not make use of the surface passivating ligands resulting in formation of surface traps as well as high bundle formation in the case of nanotubes [28]. The emission spectrum for TiO_2

nanotubes depicted in Figure 3(b) shows a narrow, sharp Gaussian peak with high intensity. The emission maximum located at 400 nm is red-shifted from the absorption band-edge. The characteristics of the observed emission spectrum are indicative of minimum bundle formation as validated by the SEM and TEM. The use of microwave as the heating source compared to the conventional heating method used in hydrothermal processes result in short synthetic time as well as high energy system that can limit the formation of bundles.

Conclusion

Highly crystalline ZnO nanorods and TiO_2 one dimensional structures were successfully synthesized via the microwave-assisted hydrothermal method. The structural properties of ZnO indicated the predominance of a hexagonal phase and growth of pointed nanorods in (100) direction. A mixed crystal phase was detected for TiO_2 with anatase, rutile and Ti_4O_7 present. The morphology was found to be tubular with diameters of approximately 25 nm. The difference in crystallinity of the two materials is ascribed to materials different size and morphology. There was also less formation of bundles thought to be as a result of the evenly distributed heat generated by the microwave. The optical properties of both ZnO and TiO_2 nanostructures showed characteristics of strong quantum confinement regime. The photoluminescence spectrum of TiO_2 nanotubes show good improvement from previously reported data.

References

1. SH Yu, J Yang, YT Qian, M Yoshimura. Optical properties of ZnS nanosheets, ZnO dendrites, and their lamellar precursor $ZnS{\cdot}(NH_2CH_2CH_2NH_2)_{0.5}$. Chemical Physics Letters. 2002; 361: 362–366.
2. J Yang, JH Zeng, SH Yu, L Yang, GE Zhou, et al. Formation process of CdS nanorods via solvothermal route. Chemistry of Materials. 2000; 12: 3259–3263.
3. JH Zhan, XG Yang, DW Wang, SD Li. Y Xie, et al. Polymer-controlled growth of CdS nanowires. Advanced Materials. 2000; 12: 1348–1351.

4. YT Chen, JB Ding, Y Guo, LB Kong, HL Li. A facile route to preparation of CdS nanorods. Materials Chemistry and Physics. 2003; 77: 734–737.
5. YW Jun, JS Choi, J Cheon. Shape control of semiconductor and metal oxide nanocrystals through nonhydrolytic colloidal routes. Angewandte Chemie International Edition. 2006; 45: 3414–3439.
6. Y Li, J Fen, S Daniels, NL Pickett, P O'Brien. A highly luminescent ZnS/CdSe/ZnS nanocrystals-tetrapeptide biolabeling agent. Journal of Nanoscience and Nanotechnology. 2007; 7: 2301–2308.
7. R Viswanatha, S Sapra, H Amenitsch, B Sartori, DD Sarma. Growth of semiconducting nanocrystals of CdS and ZnS. Journal of Nanoscience and Nanotechnology. 2007; 7: 1726–1729.
8. A Nag, S Sapra, S Chakraborty, S Basu, DD Sarma. Synthesis of CdSe nanocrystals in a noncoordinating solvent: effect of reaction temperature on size and optical properties. Journal of Nanoscience and Nanotechnology. 2007; 7: 1965–1968.
9. YP He, YM Miao, CR Li, SQ Wang, L Cao, et al. Size and structure effect on optical transitions of iron oxide nanocrystals. Physical Review B. 2005; 71, Article ID 125411.
10. C Burda, X Chen, R Narayanan, MA El-Sayed. Chemistry and properties of nanocrystals of different shapes. Chemical Reviews. 2005; 105: 1025–1102.
11. Z Ji, S Zhao, C Wang, K Liu. ZnO nanoparticle films prepared by oxidation of metallic zinc in H_2O_2 solution and subsequent process. Materials Science and Engineering B. 2005; 117: 63–66.
12. WQ Peng, SC Qu, GW Cong, ZG Wang. Structure and visible luminescence of ZnO nanoparticles. Materials Science in Semiconductor Processing. 2006; 9: 156–159.
13. XL Yuan, BP Zhang, J Niitsuma, T Sekiguchi. Cathodoluminescence characterization of ZnO nanotubes grown by MOCVD on sapphire substrate. Materials Science in Semiconductor Processing. 2006; 9: 146–150.
14. Y Sun, GM Fuge, NA Fox, DJ Riley, MNR Ashfold. Synthesis of aligned arrays of ultrathin ZnO nanotubes on a

Si wafer coated with a thin ZnO film. Advanced Materials. 2005; 17: 2477–2481.
15. J Zhou, Z Wang, L Wang, M Wu, S Ouyang, et al. Synthesis of ZnO hexagonal tubes by a microwave heating method. Superlattices and Microstructures. 2006; 39: 314–318.
16. S Polarz, AV Orlov, F Schüth, AH Lu. Preparation of high-surface-area zinc oxide with ordered porosity, different pore sizes, and nanocrystalline walls. Chemistry A European Journal. 2007; 13: 592–597.
17. HE Unalan, P Hiralal, N Rupesinghe, S Dalal, WI Milne, et al. Rapid synthesis of aligned zinc oxide nanowires. Nanotechnology. 2008; 19, Article ID 255608.
18. RF Zhuo, HT Feng, Q Liang. Morphology-controlled synthesis, growth mechanism, optical and microwave absorption properties of ZnO nanocombs. Journal of Physics D. 2008; 41.
19. H Cheng, J Cheng, Y Zhang, QM Wang. Large-scale fabrication of ZnO micro-and nano-structures by microwave thermal evaporation deposition. Journal of Crystal Growth. 2007; 299: 34–40.
20. A Fujishima, K Honda. Electrochemical photolysis of water at a semiconductor electrode. Nature. 1972; 238: 37–38.
21. AL Linsebigler, G Lu, JT Yates. Photocatalysis on TiO. Chemical Reviews. 1995; 95: 735–758.
22. A Fujishima, TN Rao, DA Tryk. Titanium dioxide photocatalysis. Journal of Photochemistry and Photobiology C. 2000; 1: 1–21.
23. LR Skubal, NK Meshkov, MC Vogt. Detection and identification of gaseous organics using a TiO. Journal of Photochemistry and Photobiology A. 2002; 148: 103–108.
24. B O'Regan, M Grätzel. A low-cost, high-efficiency solar cell based on dye-sensitized colloidal TiO. Nature. 1991; 353: 737–740.
25. R Wang, K Hashimoto, A Fujishima. Light-induced amphiphilic surfaces. Nature. 1997; 388: 431–432.
26. LM Sikhwivhilu, S Sinha Ray, NJ Coville. Influence of bases on hydrothermal synthesis of titanate nanostructures. Applied Physics A. 2009; 94: 963–973.

27. BD Yao, YF Chan, XY Zhang, WF Zhang, ZY Yang, et al. Formation mechanism of TiO_2 nanotubes. Applied Physics Letters. 2003; 82: 281–283.
28. MA Khan, HT Jung, OB Yang. Opto-electronic properties of titania nanotubes. Chemical Physics Letters. 2008; 458: 134–137.